

Cite this: *Chem. Commun.*, 2012, **48**, 4335–4337

www.rsc.org/chemcomm

COMMUNICATION

Synthesis of monolithic meso–macroporous silica and carbon with tunable pore size†

Ara Kim, Robert Black, Yong Jae Hyun, Linda F. Nazar and Eric Prouzet*

Received 5th February 2012, Accepted 12th March 2012

DOI: 10.1039/c2cc30815k

Monolithic porous silica and carbon structures have been obtained by the synthesis of silica inside the aqueous phase of a sponge-like Swollen Liquid Crystal, and the parallel preparation of carbon replica.

Porous materials are of prime importance in many reactions and processes that require a strong interaction between a solid and its environment or a controlled flow within the material. Surprisingly, if a breakthrough in material chemistry was provided for porous inorganic powders with the synthesis of mesostructured materials like MCM-41 and FSM-16,¹ major applications for these materials are still expected. In parallel, the development of monolithic porous inorganic materials did not generate the same activity, despite great successes in applications.^{2,3} This difference is certainly due to the difficulty to synthesize monolithic porous materials with a well-defined porosity, even though such materials find applications in various domains like chromatography,⁴ batteries,⁵ and more generally in the design of 3D electrodes.⁶

Among the different methods developed until now for the synthesis of porous inorganic monoliths with a controlled porosity, the most successful uses phase separation, and leads to porous silica monoliths—known as Chromolith™ columns for HPLC—and hybrid or titania materials.^{2,3} However, it is still a challenge to reach smaller pores, which could help to broaden the domain of applications like protein size-exclusion separation, or high surface porous electrodes. We describe hereinafter how 3D monolithic porous materials with a variable pore size in the meso–macroporous range (20–200 nm) are obtained by tuning first the structure of oil-in-water (O/W) hexagonal Swollen Liquid Crystals (SLC) into 3D sponge-like geometry, followed by silica condensation in the aqueous phase. We illustrate how the structure of the SLC and sol–gel parameters direct the structure of the porous silica monoliths. This method can be expanded to many structures and materials, and we illustrate it with two examples of monolithic porous silica structures and carbon replica.

Soft matter-based systems, described as hexagonal O/W SLC, can be used as adaptive matrices for the synthesis of nanomaterials shaped by either the organic or the aqueous framework.^{7,8} These mesophases are based on infinite oil cylinders hexagonally distributed within a salted aqueous medium, the cylinders being stabilized by anionic, cationic or nonionic surfactants combined with 1-pentanol used as a cosurfactant. As these systems take profit from the dynamics of soft matter, the oil cylinder diameters can easily be tuned between 3 and 30 nm. The hexagonal structure is only obtained through a fine balance between parameters:⁸

$$C_s = 0.156\rho - 0.104 \quad (1)$$

with C_s the salt ionic force equal to concentration (mol L^{-1}) for monovalent salts, and ρ the swelling volume ratio of the nonpolar medium (cyclohexane) over the aqueous medium.

These parameters must be finely adjusted to achieve the formation of the hexagonal SLC, and avoid the formation of biphasic Winsor-type phases,⁹ but a controlled variation of the components can accompany a progressive phase transition from hexagonal (H_1) to sponge-like (L_3) geometries. We used this transition to design 3D bicontinuous matrices for the preparation of porous monolithic materials. This transition can be induced either by an excess of cosurfactant, or by an excess of aqueous phase.

We demonstrate first how the excess of cosurfactant induces this transition. The evolution of the Small Angle X-ray Diffraction patterns (SAXD) is displayed in Fig. 1, for three SLCs prepared with cetylpyridinium chloride (CtPCl), and three amounts of 1-pentanol used as a co-surfactant (see also Fig. S1, ESI†). When the amount of pentanol is below the optimized value (pentanol: 0.22 g, pentanol/CtPCl = 0.27 wt), the sample is creamy and white, and a disordered structure identified by a single correlation peak at $q = 0.43 \text{ nm}^{-1}$ ($d = 14.6 \text{ nm}$) is observed, characteristic of an isotropic fluid L_3 sponge-like mesophase.¹⁰

Increasing the amount of pentanol to the optimized value for the formation of the hexagonal phase (pentanol = 0.5 g, pentanol/CtPCl = 0.43 wt) leads to a transparent and rigid gel, with a diffraction pattern characteristic of a $P6m$ hexagonal symmetry ($d_{10} = 22.5 \text{ nm}$, $q = 0.28 \text{ nm}^{-1}$; $d_{11} = 12.8 \text{ nm}$, $q = 0.49 \text{ nm}^{-1}$; $d_{20} = 11.2 \text{ nm}$, $q = 0.56 \text{ nm}^{-1}$).⁸ Adding an excess of cosurfactant (pentanol = 0.45 g, pentanol/CtPCl = 0.56 wt) gives also a transparent, but very fluidic phase identified as a sponge-like structure.

University of Waterloo and Waterloo Institute of Nanotechnology (WIN), 200 University Av. West, Waterloo, ON N2L 3G1, Canada.
E-mail: eprouzet@uwaterloo.ca; Fax: +1 519 746-0435;
Tel: +1 519-888-4567 (x38172)

† Electronic supplementary information (ESI) available: Experiments and methods; SAXS patterns of the SLC prepared with various amounts of pentanol, additional SEM pictures. See DOI: 10.1039/c2cc30815k

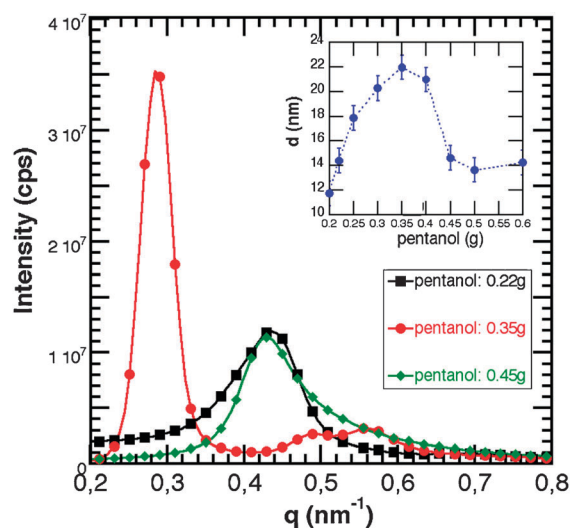


Fig. 1 Evolution of the SAXS pattern as a function of the addition of co-surfactant. Inset: evolution of the d -spacing as the function of the co-surfactant.

This phase is stable for months. As the cosurfactant over CtPCI ratio increases (Fig. 1, inset), d_{10} increases from 12 to 22 nm up to the formation of the hexagonal structure, which is only observed within a narrow concentration range (pentanol: 0.25–0.35 g, pentanol/CtPCI: 0.31–0.43 wt). Beyond this domain, as soon as a slight excess of pentanol is added, the hexagonal structure is destroyed, and a brutal transition is observed from a gel (hexagonal) to a fluidic solution (sponge-like), along with a steep decreasing of the d -spacing back to 14 nm. This sponge-like mesophase can be used for a True Liquid Crystal Templating synthesis.

The stability of a SLC is the result of a fine balance between several components, especially the O/W interface curvature, and the electrostatic ones (surfactant head charge and ionic force of water). The cosurfactant is a constitutive brick of this interface, acting like a wedge intercalated between the surfactant molecules to adjust the interface curvature. As a result, both the ionic force able to shield the surfactant head repulsion, and the O/W curvature must fit, as illustrated in eqn (1), and the amount of cosurfactant must be optimized to allow the formation of the hexagonal phase. Adding an excess of cosurfactant contributes to decrease furthermore the cylinder curvature, and modify accordingly the cylinder curvature–volume ratio. The hexagonal phase becomes unstable and the structure evolves toward a sponge-like geometry, only able to adapt the reduction in curvature resulting from the addition of pentanol.

A similar effect results from the increasing of the water–oil ratio that leads to an increasing of the inter-cylinder distances, and their concomitant destabilization.

The structural evolution is more difficult to follow as resulting correlation distances are out of range of laboratory SAXS equipment, but it provides the aqueous phase required for the synthesis of continuous solid frameworks. Therefore, we used this second mechanism to synthesize a monolithic porous silica, the silica structure being the “memory” of the initial aqueous phase in the sponge-like SLC, and the porosity that of the organic one.

Preparation of silica porous monoliths used a method that integrates sol–gel, mesoporous material synthesis and liquid

crystals properties into a synergistic reaction mechanism.¹¹ The silica precursor was based on the nonionic PEO-based silica hybrid micelles developed for the preparation of MSU mesoporous silica.^{12,13} The silica–surfactant precursor solution is used as the aqueous phase of the SLC, and silica condensation is catalysed by sodium fluoride, added in total (referred as 100%) or partial (referred as $x\%$) substitution of NaCl as a stabilizing salt of the SLC (see ESI†). The silica condensation is induced by both the confinement and catalyst concentration, and, unlike what is observed with the synthesis of mesoporous MSU silica,^{12,13} where the nonionic surfactant is trapped within the silica and creates the mesoporosity upon calcination, the confined reaction in SLCs expels the surfactant from the silica framework to the organic part. It results that the silica structure itself is dense, but its shape is controlled by the sponge-like structure used as a confinement matrix.

The SLCs are dynamic and adaptive matrices, and their structure can be modified beforehand or adapt to changes in the reactional medium during the synthesis. We have identified several factors that can control the final silica structure, and we illustrate in the present communication how the temperature of synthesis and NaF percentage can be combined to obtain different porosity by starting from the same system. These two parameters have an independent effect on the silica condensation reaction: the temperature increases the kinetics by increasing the energy, whereas the catalyst enhances the silica oxolation reaction.¹² It results that both of them act in parallel and influence a “spinodal-like” phase separation between the inorganic framework and the organic phase. As the kinetic is enhanced, the resulting silica will be denser and thicker, which induces the same structure for the remaining organic network. We prepared a series of SLCs with different NaCl:NaF ratios and carried out the reaction at different temperatures (see ESI†). As a result, we observed (Fig. 2, and Fig. S2 and 3, ESI†) that the pore size increases from low temperature/low NaF% (top-left) to high temperature/high NaF% (bottom-right).

Such silica structures (see Fig. S4, ESI†) were used for the preparation of carbon replica by the resorcinol method (ESI†). Two examples of porous carbon are illustrated in Fig. 3 (see also Fig. S5, ESI†). Carbon prepared from silica with the largest pore size (high amount of NaF, Fig. 3a and b) exhibits a good and continuous porous structure, and this

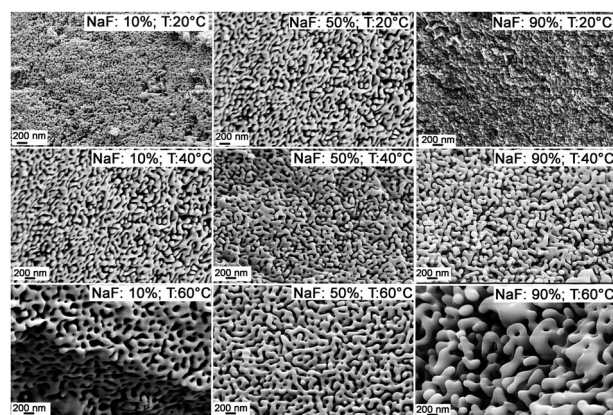


Fig. 2 SEM pictures of silica sponge-like structures prepared with different amounts of NaF, and at different temperatures.

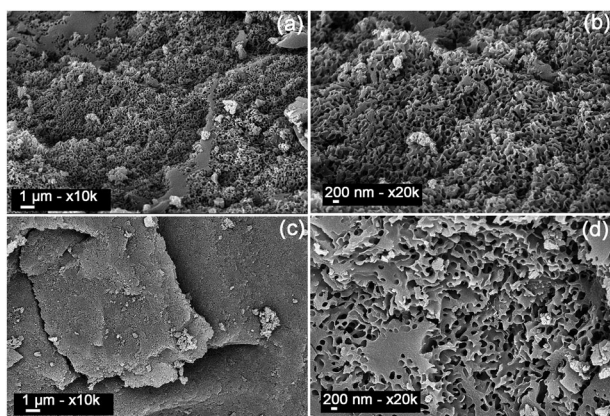


Fig. 3 SEM pictures of the carbon replica of sample A prepared with 80% NaF and 20% NaCl (a, b), and sample B prepared with 20% NaF and 80% NaCl (c, d).

material presents a specific surface area equal to $340 \text{ m}^2 \text{ g}^{-1}$, most of it being microporous surface ($240 \text{ m}^2 \text{ g}^{-1}$ measured by the t -plot analysis). With a smaller initial pore size, a heterogeneous structure was obtained (low amount of NaF, Fig. 3c and d), probably because the initial pore size was too small to allow a good expansion of the carbon structure. We conclude that the silica obtained by the synthesis in sponge-like SLCs can be easily used as a mould for carbon replica if the pore size of silica remains above a minimum value, to prevent any pore cloaking during the carbon reaction.

This work was supported by the “Transformational Nanoscale Technologies for High Capacity Energy Storage” project, funded by the Strategic Projects Grants of the Canadian NSERC Agency.

Notes and references

1 C. T. Kresge, M. E. Leonowicz, W. J. Roth, J. C. Vartuli and J. S. Beck, *Nature*, 1992, **359**, 710; S. Inagaki, Y. Fukushima and K. Kuroda, *J. Chem. Soc., Chem. Commun.*, 1993, 680.

2 K. Nakanishi and K. Kanamori, *J. Mater. Chem.*, 2005, **15**, 3776; T. Amatani, K. Nakanishi, K. Hirao and T. Kodaira, *Chem. Mater.*, 2005, **17**, 2114; K. Nakanishi and N. Nobuo, *Acc. Chem. Res.*, 2007, **40**, 863; K. Kanamori, K. Nakanishi and T. Hanada, *Soft Matter*, 2009, **5**, 3106.

3 J. Konishi, K. Fujita, K. Nakanishi and K. Hirao, *Chem. Mater.*, 2006, **18**, 6069; J. Konishi, K. Fujita, K. Nakanishi, S. Nishitsuji, M. Takenaka, K. Miura and K. Hirao, *J. Sol-Gel Sci. Technol.*, 2008, **46**, 63; J. Konishi, K. Fujita, K. Nakanishi, K. Hirao, K. Morisato, S. Miyazaki and M. Ohira, *J. Chromatogr., A*, 2009, **1216**, 7375; G. Hasegawa, K. Kanamori, K. Nakanishi and T. Hanada, *J. Ceram. Soc. Jpn.*, 2010, **93**, 3110.

4 D. R. Bunch and S. Wang, *J. Sep. Sci.*, 2011, **34**, 2003; H. D. Qiu, X. J. Liang, M. Sun and S. X. Jiang, *Anal. Bioanal. Chem.*, 2011, **399**, 3307; D. Wistuba, *J. Chromatogr., A*, 2010, **1217**, 941.

5 D. R. Rolison and L. F. Nazar, *MRS Bull.*, 2011, **36**, 486.

6 T. S. Arthur, D. J. Bates, N. Cirigliano, D. C. Johnson, P. Malati, J. M. Mosby, E. Perre, M. T. Rawls, A. L. Prieto and B. Dunn, *MRS Bull.*, 2011, **36**, 523; R. W. Hart, H. S. White, B. Dunn and D. R. Rolison, *Electrochem. Commun.*, 2003, **5**, 120.

7 G. Surendran, M. Tokumoto, E. Pena dos Santos, H. Remita, L. Ramos, P. J. Kooyman, C. V. Santilli, C. Bourgaux, P. Dieudonné and E. Prouzet, *Chem. Mater.*, 2005, **17**, 1505; G. Surendran, G. Apostolescu, M. Tokumoto, E. Prouzet, L. Ramos, P. Beaunier, P. J. Kooyman, A. Etcheberry and H. Remita, *Small*, 2005, **1**, 964; G. Surendran, L. Ramos, B. Pansu, E. Prouzet, P. Beaunier, F. Audonnet and H. Remita, *Chem. Mater.*, 2007, **19**, 5045; G. Surendran, F. Ksar, L. Ramos, B. Keita, L. Nadjo, E. Prouzet, P. Beaunier, P. Dieudonné, F. Audonnet and H. Remita, *J. Phys. Chem. C*, 2008, **112**, 10740; F. Ksar, L. Ramos, B. Keita, L. Nadjo, P. Beaunier and H. Remita, *Chem. Mater.*, 2009, **21**, 3677.

8 E. Pena dos Santos, M. Tokumoto, G. Surendran, H. Remita, C. Bourgaux, P. Dieudonné, E. Prouzet and L. Ramos, *Langmuir*, 2005, **21**, 4362.

9 P. A. Winsor, *Chem. Rev.*, 1968, **68**, 1.

10 R. Gomati, N. Bouguerra and A. Gharbi, *Physica B*, 2001, **299**, 101.

11 R. Backov, *Soft Matter*, 2006, **2**, 452; E. Prouzet, S. Ravaine, C. Sanchez and R. Backov, *New. J. Chem.*, 2008, **32**, 1284.

12 C. Boissière, A. Larbot, C. Bourgaux, E. Prouzet and C. A. Bunton, *Chem. Mater.*, 2001, **13**, 3580; E. Prouzet and C. Boissière, *C. R. Chim.*, 2005, **8**, 579.

13 D. Ortiz de Zarate, F. Bouyer, H. Zschiedrich, P. J. Kooyman, P. Trens, J. Lapichella, R. Durand, C. Guillem and E. Prouzet, *Chem. Mater.*, 2008, **20**, 1410.